

N-Type Doping of Gallium Antimonide and Aluminum Antimonide Grown by Molecular Beam Epitaxy using Lead Telluride as a Tellurium Dopant Source

S. SUBBANNA, G. TUTTLE and H. KROEMER

Department of Electrical and Computer Engineering,
University of California, Santa Barbara, CA 93106.

Lead telluride was used as a "captive" source of tellurium (Te) for the *n*-type doping of gallium antimonide (GaSb) and aluminum antimonide (AlSb) grown by molecular beam epitaxy. Controllable carrier concentrations from 1.2×10^{16} to $1.6 \times 10^{18} \text{ cm}^{-3}$ were obtained. High room-temperature Hall mobilities of $4200 \text{ cm}^2/\text{V} \cdot \text{s}$ were measured for the low-doped GaSb samples. In the growth temperature range of interest, doping efficiencies are approximately 50% of those in GaAs. For GaSb, SIMS data show that the Te incorporation decreases significantly at growth temperatures above 500°C . However, in AlSb, there is no significant reduction in the incorporation of Te up to at least 650°C . In contrast, the Te incorporation into AlSb decreases at *low* temperatures. There is also some evidence of surface segregation in AlSb. Contrary to other doping studies, increasing the Sb:Ga flux ratio was found to *reduce* the Te incorporation.

Key words: Gallium antimonide, aluminum antimonide, MBE, tellurium doping

INTRODUCTION

The *n*-type doping behavior of the two antimonides GaSb and AlSb by molecular beam epitaxy (MBE) is quite different than that of the arsenides. Silicon and tin, the two donors of choice for MBE-grown GaAs, are partially compensated acceptors in GaSb¹ and AlSb.² Hence a column-VI chalcogenide element, like S, Se or Te, must be used for *n*-type doping.

One of the principal problems with the column-VI elements is the decrease in dopant incorporation with increasing growth temperature. This loss of dopant is quite severe at the normal growth temperatures used for GaAs. This is one of the reasons why Si and Sn have been preferred over the chalcogenides for *n*-type doping of MBE-grown GaAs. Because of the lower growth temperature of antimonides, decrease in incorporation is less severe there, but it remains important. The problem is least severe for Te, hence making it the *n*-type dopant of choice for GaSb and AlSb.

Using an elemental Te source for doping MBE-grown GaSb, Yano *et al.*³ have reported carrier concentrations in the range 5×10^{17} to $1 \times 10^{18} \text{ cm}^{-3}$. Mobilities were less than $2000 \text{ cm}^2/\text{V} \cdot \text{s}$. However, elemental Te is a difficult dopant to control, for two reasons: (a) There is a strong chemical reaction of Te at the surface with Ga. (b) The low operating temperature of an elemental tellurium source, in the $200\text{--}250^\circ \text{C}$ range, introduces severe restrictions on the bakeout of the vacuum system, to avoid the massive redistribution of Te throughout the vacuum system, which can result in a high system background doping, including cross contamination of other sources.

One alternate attempt at *n*-type doping of GaSb,

with sulfur, has used H_2S gas as the sulfur source.⁴ But the incorporation of sulfur was found to be extremely inefficient, and maximum carrier concentrations of only $4 \times 10^{16} \text{ cm}^{-3}$ were obtained. Low mobilities of about $2000 \text{ cm}^2/\text{V} \cdot \text{s}$ were reported. Furthermore, sulfur was found to be an undesirably deep donor with an activation energy of 75 meV, a circumstance that contributes to the low carrier concentration. An alternate doping attempt, using selenium, has involved the electrochemical generation of the column-VI element from its silver salt,⁵ similar to previous work⁶ on doping GaAs in this fashion, but no details are available on the results for GaSb.

In the growth of GaAs, one of the least troublesome methods to achieve *n*-type doping with column-VI elements has been the use of PbS, PbSe or PbTe as a "captive source" of the chalcogen,⁷ in which the doping element forms a compound with lead. The source evaporates in molecular form, with little decomposition. On the substrate, the molecule decomposes, and the chalcogen is incorporated, while the lead evaporates. Doping levels of $2 \times 10^{19} \text{ cm}^{-3}$ were achieved⁸ by doping GaAs with PbTe at a substrate temperature of 530°C . The main problem with these captive sources continues to be a substantial loss of the column-VI donors at the temperatures required for growth of high-quality GaAs and (Al,Ga)As (600°C or greater), leading to problems with controllability and reproducibility. Hence, this approach has not been widely adopted for the arsenides, where the use of Si and Sn are more attractive alternatives.

Considering that these more attractive alternatives do not exist with GaSb and AlSb, and that the dopant loss problems should be somewhat less severe on these materials with their lower growth temperature, the otherwise promising lead chalcogenide results on GaAs led us to investigate Te dop-

ing of GaSb using a PbTe source, and to extend these studies further to AlSb. The present paper describes the results of these studies. Carrier concentrations were determined using van der Pauw measurements, at room-temperature and liquid nitrogen temperature. To determine elemental tellurium levels, as opposed to carrier concentration, SIMS studies were also carried out.

We had chosen PbTe over PbSe for our work, principally because of its anticipated lower evaporation rate. While our work was in progress, similar work using PbSe rather than PbTe source was reported by McLean *et al.*⁹ These authors achieved doping levels from 1×10^{16} to $5 \times 10^{17} \text{ cm}^{-3}$, along with room temperature mobilities up to $4100 \text{ cm}^2/\text{V}\cdot\text{s}$ for the low-doped samples. However, Se re-evaporation was a severe problem, and in order to achieve the reported doping levels, extremely high Sb:Ga atomic flux ratios ($>40:1$) had to be used. Even at these high flux ratios, evaporation of the entire incoming dopant from the surface took place for temperatures above 530°C . Inasmuch as *low* flux ratios are necessary for growth of high-quality GaSb and AlSb, an even poorer dopant incorporation should be expected for high-quality layers. The same authors also reported that the doping efficiency was very low (1–10%) compared to GaAs.¹⁰ Last, but not least, selenium appears to be an undesirably deep donor in GaSb,¹¹ similar to sulfur. As we shall see, the results with PbTe appear less troublesome than those achieved with PbSe.

EXPERIMENTAL

The PbTe source was prepared by melting together a mixture of PbTe as obtained from the supplier (Alfa Ventron), with an added excess of lead about 10% by weight. The melt, prepared in an evacuated quartz ampoule, was cooled slowly from about 950°C until it solidified, and then loaded into graphite crucible, which was placed in a downward-looking furnace in the MBE machine. The reason for this source preparation, as pointed out by Sheng *et al.*,⁸ is to ensure that the PbTe source material is lead-saturated. For such a source, the main molecular species has shown to be PbTe, with the flux of Te-dimers more than an order of magnitude lower.¹² This helps prevent a surface reaction between the elemental Te and the Ga at the surface forming gallium telluride (Ga_2Te or Ga_2Te_3), which has been shown to complicate the growth.¹³

All samples were grown by molecular beam epitaxy in a Varian MBE-360 machine. Elemental sources were used for Ga, Al and Sb, the latter producing Sb_4 . The GaSb and AlSb growth rates were calculated from Ga and Al fluxes obtained from GaAs and AlAs RHEED oscillations, and also by measuring the thicknesses of layers grown. The growth rate was set at $0.5 \mu\text{m/hr}$ (both GaSb and AlSb) for all the samples used for electrical measurements, and for some of the SIMS samples. No systematic attempt was made to study dopant incorporation as a function of growth rate.

The Sb flux was calibrated by observing the stabilization change of the RHEED pattern on AlSb at 550°C , as follows. By fixing the Sb flux and slowly increasing the Al flux during the growth of AlSb, a point will be reached at which the growth will change from (3×1) Sb-stable growth to (4×2) Al-stable growth. The Sb flux arriving at the surface is then just barely insufficient to maintain Sb-stable growth: continued Al-stable growth under such conditions leads to the accumulation of excess aluminum. As the substrate temperature is decreased to 550°C , the Sb flux required just to maintain stabilization at the crossover point (for a given Al flux) reaches an asymptotic lower limit, below which no AlSb growth is possible. If one assumes that at sufficiently low temperatures only stoichiometric excess Sb will re-evaporate, then this asymptotic Sb flux should be equal to the Al flux, which is easily determined from the measured growth rate. We therefore express all flux ratios in this paper as *effective* flux ratios, relative to the ratio at the 550°C stability crossover point.

An independent estimate of the *true* atomic Sb flux arriving at the substrate was made by measuring the thickness of an elemental Sb film deposited on a heat-cleaned GaAs substrate at room temperature. We found that the effective atomic flux ratio of 1:1 corresponds, within the limits of accuracy of the data, to a true atomic flux ratio of 1:1, implying that all the antimony atoms that arrive at the surface are able to incorporate in the growing layer. This is in contrast to the case of As_4 in the growth of GaAs, where at most 50% of the incoming As atoms are able to incorporate in the growing layer.¹⁴ We believe this high incorporation efficiency for Sb_4 is due to the cracking of Sb_4 at the substrate surface to Sb_2 at a temperature of 550°C , in which case all the incoming Sb atoms can get incorporated in the layer.¹⁴

Semi-insulating, chromium-doped GaAs substrates were used for all van der Pauw samples. In all cases the first layer was a 40 nm (or thicker) layer of AlSb, grown at 570°C . The RHEED pattern initially turned spotty, indicating 3-dimensional nucleation, probably due to the large (7%) lattice mismatch between GaAs and AlSb. However, the RHEED pattern recovered within about 15 nm to show a streaky 3×1 reconstruction. Layers grown using this nucleation procedure were mirror-smooth. The AlSb layers showed few visible defects under the microscope, while the GaSb layers showed defects ($5,000\text{--}10,000 \text{ defects/cm}^2$) that looked similar to oval defects on MBE-grown GaAs.

Following the initial nucleation, a $0.5 \mu\text{m}$ buffer layer of undoped AlSb buffer was grown at the relatively low growth temperature (for AlSb) of 520°C . Such a layer is semi-insulating; its purpose was to electrically isolate the GaSb epitaxial layer from the substrate. More than 10 V can be applied across this layer in the dark, with less than 1 mA/cm^2 flowing. In addition, this AlSb buffer layer takes up the 7% lattice mismatch between GaAs and GaSb/AlSb, and allows the GaSb to be grown on a closely lattice-

matched layer (0.8% lattice mismatch), resulting in good layer uniformity and higher mobility. Ohmic contacts to the low-doped *n*-type GaSb layers and to all the AlSb layers were obtained by alloying Au-Te dots at 350° C for 60 sec. Ohmic contacts to undoped *p*-type and highly doped *n*-type layers were obtained by alloying Au at 350° C.

Van der Pauw measurements of GaSb layers were carried out using circular etched mesas, both at room temperature and immersed in boiling liquid nitrogen. A magnetic field of 5 kG was employed. For the AlSb samples, cleaved samples about 7 mm on a side were used. SIMS measurements were carried out at Charles Evans and Associates, Redwood City, CA.

RESULTS AND DISCUSSION

Table 1 shows the raw van der Pauw data obtained for the various samples. In order to analyze the data from the van der Pauw measurements for GaSb, a two-band model of conduction is necessary. The L-valleys of GaSb, which have a high density of states and a low mobility, lie close in energy to the central Γ -minimum. The nominal electron concentration obtained from the measured Hall-coefficient ($n = 1/e|R_H|$) is neither the Γ -valley electron concentration nor the total electron concentration, but falls somewhere in between. Similarly, the nominal carrier mobility obtained from the measured Hall coefficient and measured conductivity ($\mu_H = |R_H|\sigma$) is a weighted average of the Γ -valley mobility and the L-valley mobility. To obtain a *true* electron concentration, needed for a meaningful interpretation of the data, it is necessary to sepa-

rate the contributions of the two valleys. This also yields a value for the Γ -valley mobility, which is of interest as an indicator of the overall crystal quality. In order to obtain an estimate of the number of electrons in the Γ -valley and their mobility, as well as the total electron concentration, we have assumed the following parameters, based on the literature:¹⁵ (i) A separation between Γ and L valleys $\Delta = 90$ meV at room temperature, at the upper end of the literature range; (ii) a mobility ratio $\mu_\Gamma/\mu_L = 5$; and (iii) a density-of-states ratio $N_c(L)N_c(\Gamma) = 40$, at the lower end of the literature range. The limiting values for Δ and for the density-of-states ratio were chosen to avoid over-estimating the Γ -valley mobilities and thereby the quality of the material. Table 2 shows the carrier concentration and mobility in the two valleys calculated from this model, both at room temperature and at liquid nitrogen temperature, for two typical samples. The apparent increase in carrier concentration at liquid nitrogen temperature is clearly unphysical, indicating that the model is too simple. A more complex model would take into account the highly degenerate nature of the two bands at liquid nitrogen temperature, and the possibility of impurity band conduction, and would allow us to determine the value of parameters such as Δ by requiring self-consistency.¹⁵ However, no attempt at a further refinement of the model was made.

The *total* donor concentration was estimated by adding to the total electron concentration the estimated background acceptor concentration (2.5×10^{16} cm⁻³, the value obtained for typical non-intentionally doped GaSb layers, which are inevitably *p*-type).

An Arrhenius plot of the carrier concentration (corrected for the *p*-type background concentration)

Table 1. Results of van der Pauw Measurements on all Te-doped Samples; Raw Data, not Separated into Γ - and L-valley Contributions.

$1000/T_{Te}$ (K ⁻¹)	N_{meas} (cm ⁻³) (RT)	μ_{meas} (cm ² /V-s) (RT)	N_{meas} (cm ⁻³) (LN ₂)	μ_{meas} (cm ² /V-s) (LN ₂)	Comments
GaAs					
1.555	4.3×10^{17}	4900	—	—	(all at 520° C)
1.435	4.3×10^{17}	3170	—	—	1 μ m/hr.; Hall
1.508	3.6×10^{17}	2970	—	—	1 μ m/hr.; Hall
GaSb					
1.430	2.5×10^{17}	3830	—	—	0.5 μ m/hr.; vdP
1.546	5.0×10^{15}	1085	—	—	(all at 520° C)
1.565	1.2×10^{16}	4160	1.6×10^{16}	5230	1.25 μ m/hr.; Hall
1.508	7.4×10^{16}	4000	1.25×10^{17}	6000	1 μ m/hr.; Hall
same growth	7.3×10^{16}	3870	1.2×10^{17}	5600	0.5 μ m/hr.; vdP
1.391	7.7×10^{17}	1840	1.05×10^{18}	3465	0.5 μ m/hr.; vdP
same growth	9.1×10^{17}	1680	1.25×10^{18}	3100	0.5 μ m/hr.; vdP
1.558	1.5×10^{16}	4490	2.2×10^{16}	5890	0.5 μ m/hr.; vdP
1.227	1.6×10^{18}	950	1.8×10^{18}	1475	0.5 μ m/hr.; vdP
same growth	1.55×10^{18}	940	1.85×10^{18}	1400	0.5 μ m/hr.; vdP
AlSb					
1.433	6×10^{17}	55	—	—	(all at 0.55 μ m/hr.)
1.433	6.9×10^{17}	24	—	—	650° C; vdP
1.433	6×10^{17}	65	—	—	600° C; vdP
1.433	9×10^{17}	45	—	—	550° C; vdP
1.486	2×10^{17}	—	—	—	500° C; vdP
					500° C; C-V

Table 2. Electron Concentration and Mobility Obtained from the Two Band Model for Two Samples of n-GaSb:Te. Note that the Total Electron Concentration Appears to Change Considerably for Sample #228. This is a Consequence of the Inadequacy of the Model (see Text).

Sample #	Meas. Temp.	N_T (cm^{-3})	μ_T ($\text{cm}^2/\text{V}\cdot\text{s}$)	N_L (cm^{-3})	μ_L ($\text{cm}^2/\text{V}\cdot\text{s}$)	N_T (cm^{-3})
230	RT	1.0×10^{16}	5360	1.3×10^{16}	1070	2.3×10^{16}
	LN ₂	2.1×10^{16}	6050	0.4×10^{16}	1210	2.5×10^{16}
228	RT	5.0×10^{16}	4800	6.0×10^{16}	960	1.1×10^{17}
	LN ₂	0.6×10^{17}	7800	1.5×10^{17}	1560	2.1×10^{17}

as a function of PbTe source temperature is given in Fig. 1. Data for both GaSb and AlSb are shown. The doping efficiency in GaSb at 520° C and in AlSb is about 50% of that in GaAs at 520° C. Above $1 \times 10^{18} \text{ cm}^{-3}$, the concentration flattens out, and does not go above $2 \times 10^{18} \text{ cm}^{-3}$. the slope of a line drawn through the lower data points corresponds to an activation energy of 1.6eV. This value of the activation is the same as that obtained by Sheng *et al.*⁸ for PbTe doping of GaAs at 535° C. However, the value is much lower than the activation energy of about 2.3 eV obtained from an Arrhenius plot of the vapor pressure.¹⁶ This indicates a complicated dopant incorporation mechanism, in which the arrival of PbTe molecules at the growing surface is not the rate-limiting step, and which occurs in both GaAs

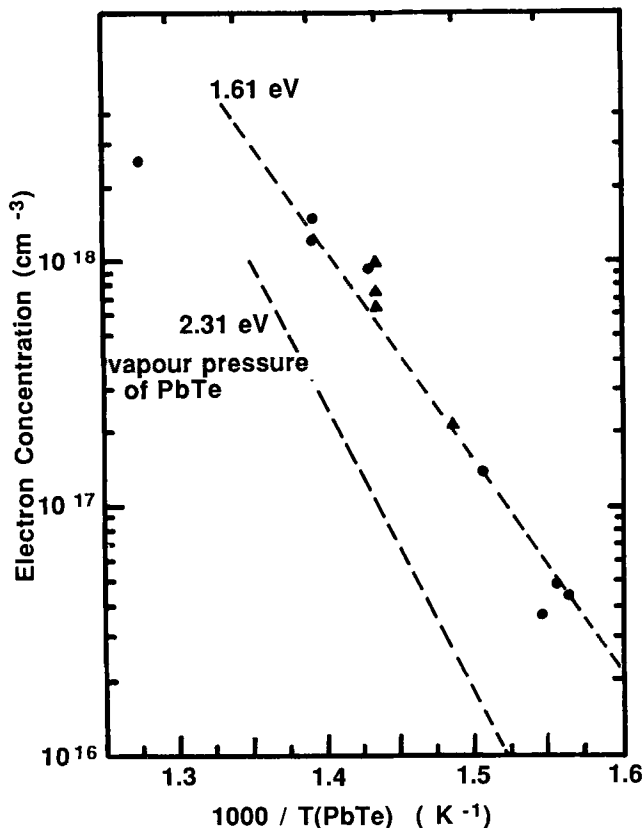


Fig. 1 — Arrhenius plot of the donor concentration (calculated using the procedure and model described in the text) as a function of PbTe source temperature, corrected for background doping. Circles are data points for GaSb layers, while triangles are data points for AlSb layers. Note the point at $2.6 \times 10^{18} \text{ cm}^{-3}$, indicating a sharp falloff from the straight line at higher doping.

and GaSb. In the case of PbSe doping of GaAs, studied by McLean *et al.*,⁹ the slope of the doping concentration vs. temperature graph was the same as that of the vapor pressure vs. temperature graph, indicating a simpler doping mechanism, in which every molecule of PbSe arriving at the surface results in one Se atom being incorporated in the growing layer. Possibly, the incorporation of lead, as well as a dependence of doping efficiency on growth parameters, may also give rise to the different activation energies.

Room temperature *raw* Hall mobilities for *n*-type GaSb layers varied from 950 to 4500 $\text{cm}^2/\text{V}\cdot\text{s}$, corresponding to Γ -valley mobilities of 1330 to 5400 $\text{cm}^2/\text{V}\cdot\text{s}$. Fig. 2 is a plot of mobility against electron concentration, also containing some earlier results. As can be seen, the Γ -valley mobilities are higher than for previous reports, indicating a better quality of the material grown. However, the highest Γ -valley mobility achieved, 5360 $\text{cm}^2/\text{V}\cdot\text{s}$, is still much lower than the *calculated* lattice mobility, which is 15,000 $\text{cm}^2/\text{V}\cdot\text{s}$. This may be due to the fact that a GaAs substrate was used. While the quality of the GaSb layer is much improved over previous *n*-type layers, it is probably not as good as layers grown on GaSb substrates. At 77 K, mobilities up to 6000 $\text{cm}^2/\text{V}\cdot\text{s}$ were measured, corresponding to Γ -valley mobility of 7800 $\text{cm}^2/\text{V}\cdot\text{s}$. In the case of AlSb, the Hall mobilities were typically 100 $\text{cm}^2/\text{V}\cdot\text{s}$.

On one high-mobility sample, variable-tempera-

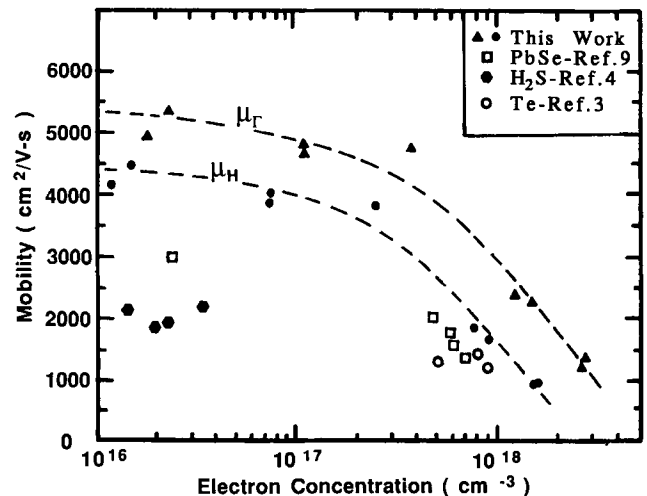


Fig. 2 — Mobility against carrier concentration for n-GaSb:Te, at 300 K. Both Hall and Γ -valley mobilities are shown. Some earlier results are plotted for comparison.

ture van der Pauw measurements were made. Fig. 3 is a plot of the raw Hall mobility and Hall concentration as functions of temperature. As can be seen, there is an increase in the *apparent* carrier concentration, as well as an apparent large rise in the *apparent* mobility, as the temperature decreases below 300 K. This is a consequence of most of the electrons collecting in the higher mobility Γ -valley. It appears that the 77 K mobility is a better estimate of the Γ -valley mobility, which is itself a better indicator of sample quality than the *raw* room-temperature Hall mobility.

In addition to the van der Pauw measurements, extensive SIMS studies were carried out to determine Te incorporation as a function of growth conditions, shown in Figs. 4 through 8. The secondary ion counts have not been converted to actual concentrations, for lack of accurate relative sensitivity factors for this material.

The results for GaSb, as a function of growth temperature, are shown in Fig. 4. A substantial decrease in Te incorporation occurs above 500° C. The loss mechanism could be due to re-evaporation of molecular PbTe before it decomposes on the GaSb surface, or possibly due to the evaporation of volatile Ga₂Te.

In contrast to the behavior reported by MacLean *et al.*⁹ for Se doping using PbSe, the incorporation rate of Te into GaSb was found to decrease slightly with increasing Sb flux, as shown in Fig. 5 for two layers grown at 520° C using two different flux ratios. Presumably, as the antimony flux increases, the competition for Sb-sites favors antimony over Te, and the Te is lost as volatile Ga₂Te before it has a chance to incorporate.

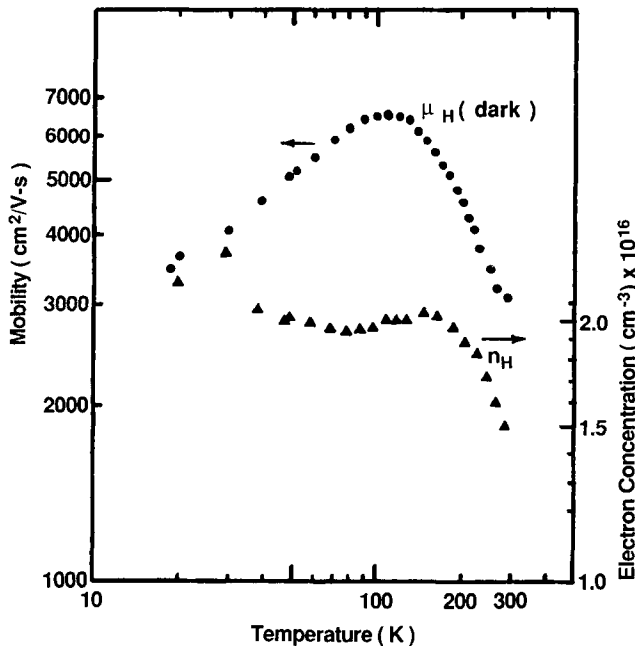


Fig. 3 — Raw Hall mobility and raw electron concentration as functions of temperature, for one sample of Te-doped GaSb. Note the steep rise in Hall mobility (and apparent carrier concentration) below room temperature, indicative of the electron transfer from the low-mobility L-valley to the high-mobility Γ -valley.

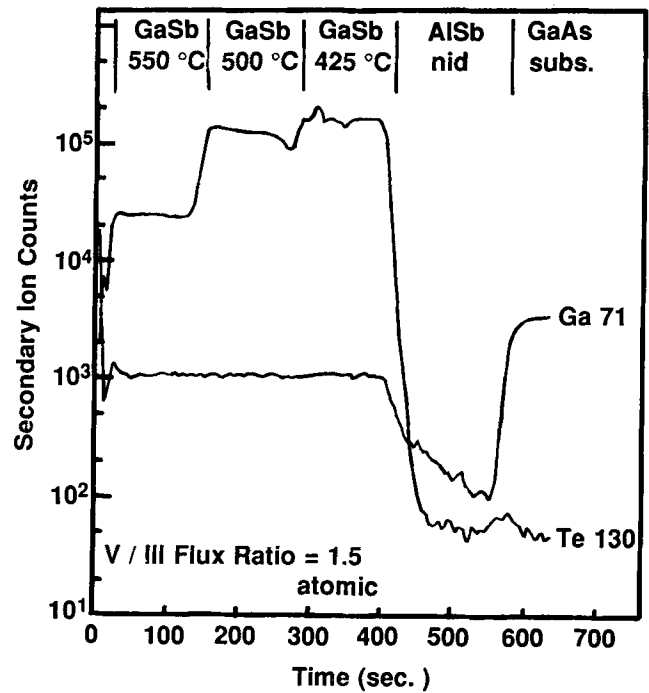


Fig. 4 — Tellurium incorporation as a function of GaSb growth temperature, as measured by SIMS. The layer structure is shown at the top of the figure. Each GaSb layer grown at a different substrate temperature was 0.5 μ m thick.

The results for AlSb, shown in Fig. 6, are quite different than those for GaSb. No loss of Te was observed up to 650° C, the highest substrate temperature investigated. This is in agreement with the observation by Andrews *et al.*,¹⁷ who found a higher

Tellurium Incorporation in GaSb as a Function of Flux Ratio (SIMS)

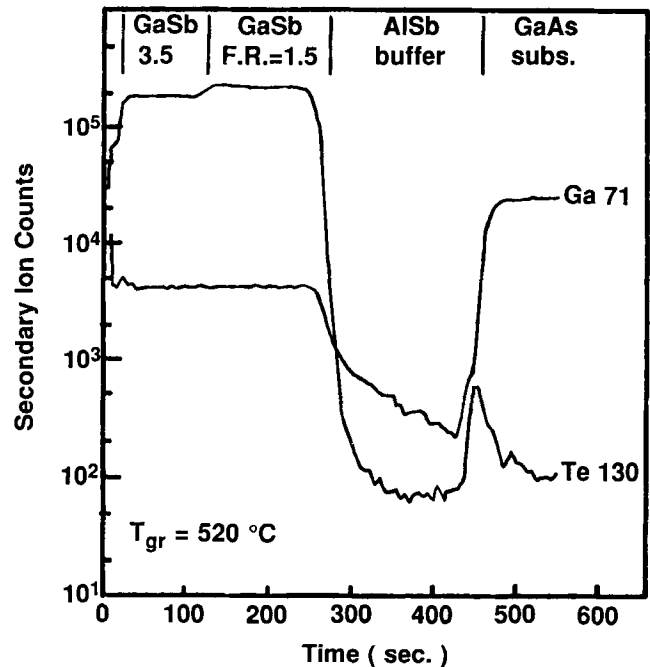


Fig. 5 — Tellurium incorporation in GaSb as a function of Sb/Ga flux ratio, as measured by SIMS. Atomic flux ratios are marked on the figure. Each GaSb layer was 0.5 μ m thick.

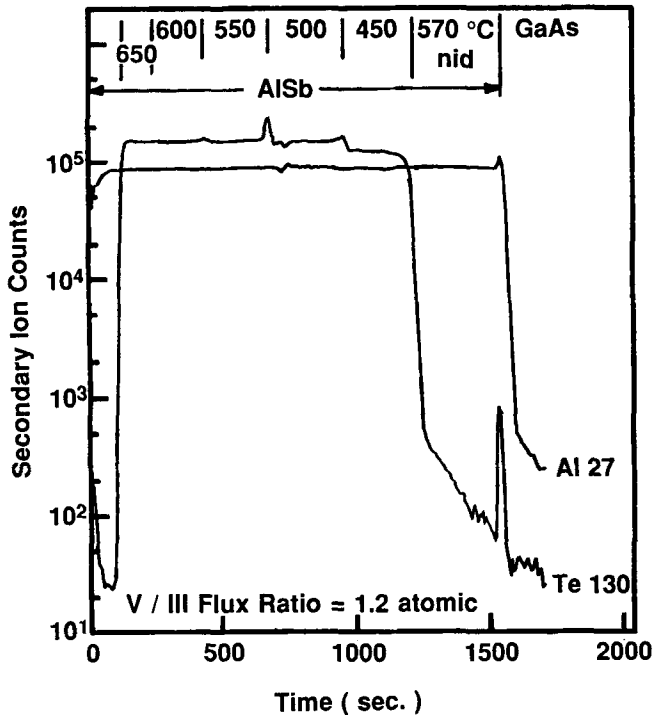


Fig. 6 — Tellurium incorporation as a function of AlSb growth temperature, as measured by SIMS. Each AlSb layer was nominally $0.75 \mu\text{m}$ thick. There was also a 75 nm undoped GaSb cap layer.

retention of S and Se in (Al,Ga)As than in GaAs. They attributed this to the much lower volatility of the aluminum chalcogenides $\text{Al}_2\text{S}/\text{Al}_2\text{S}_3$ (or $\text{Al}_2\text{Se}/\text{Al}_2\text{Se}_3$) compared to the gallium chalcogenides. This mechanism is evidently also present in our doping

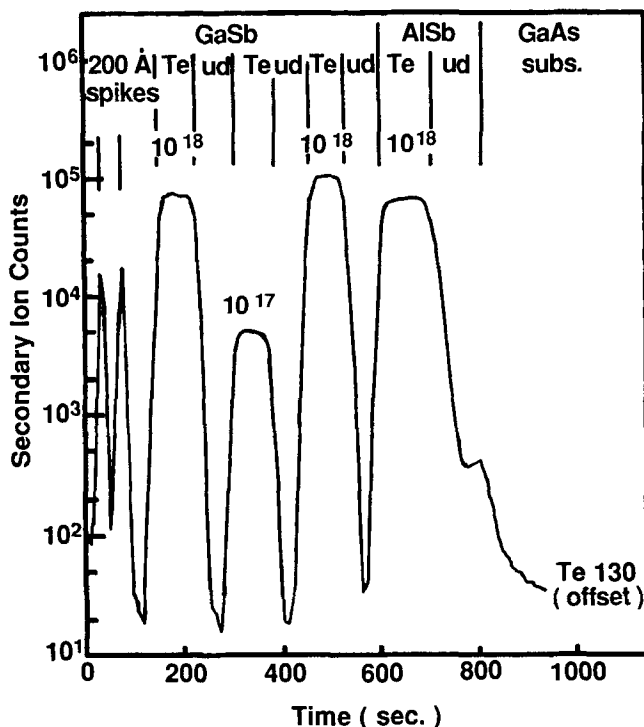


Fig. 7 — Doping spikes and transients in GaSb and AlSb, as measured by SIMS. Each of the doped (and undoped) layers was $0.5 \mu\text{m}$ thick. Note the sharp doping spikes near the surface (see text).

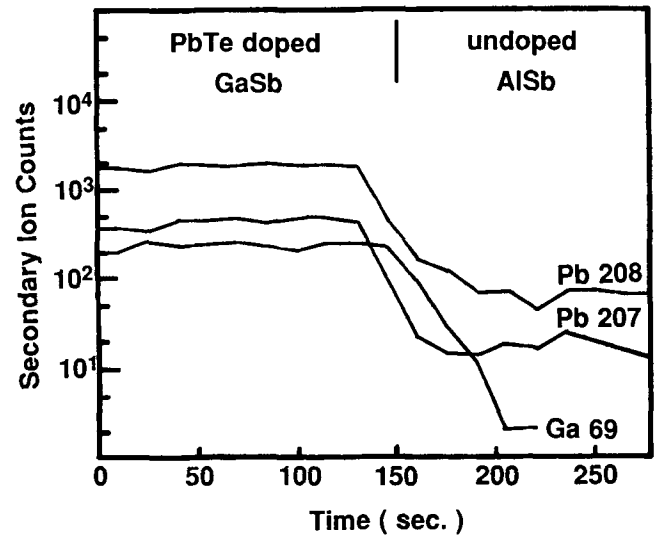


Fig. 8 — Lead incorporation in heavily Tellurium-doped GaSb, as measured by SIMS. Note the presence of a lead signal in the undoped AlSb buffer layer, which is above the background level (see text). The GaSb layer was $0.5 \mu\text{m}$ thick.

experiments. If correct, this interpretation would imply that the falloff in GaSb is due to gallium telluride formation and evaporation.

A surprising observation was that in AlSb the Te incorporation slightly *decreases* at the lowest growth temperature investigated, 450°C . This is in contrast to GaSb, which shows an increase in incorporation at this temperature (Fig. 4). The reason for the peculiar drop in the Te incorporation into AlSb at low temperatures is not clear; it may reflect a true drop in solid solubility for Te in AlSb with decreasing temperature. In addition, at temperatures below 600°C , there occur Te-spikes in the continuous growth of AlSb when the temperature is suddenly raised. The latter indicates some surface segregation of Te on AlSb at the lower growth temperatures: as the temperature is raised, the steady-state Te surface concentration evidently drops, and the excess Te is incorporated into the growing layer at this point.

To see whether or not the presence of some surface segregation of Te in AlSb might cause a problem in obtaining sharp doping profiles, a SIMS study of Te-doped layers and doping spikes was carried out (Fig. 7). There was no variation of incorporation across the doped layers, indicating that surface segregation does not play a major role. In addition 20 nm doping spikes were grown. These spikes are symmetric and show only diffusion broadening, of the order of 100 nm . These results indicate that it should be possible to obtain sharp doping profiles in both GaSb and AlSb. At present, the limitation is the slow time-response of the PbTe source (tens of minutes), due to its large thermal mass.

The incorporation of lead into heavily doped GaSb is shown in Fig. 8. The particular sample was grown with a high PbTe flux corresponding to a doping of $1 \times 10^{19} \text{ cm}^{-3}$, but the actual carrier concentration was only $2.6 \times 10^{18} \text{ cm}^{-3}$. The SIMS data indicate that there is Pb incorporation, but we cannot make

an accurate estimate of the actual level. However, there is also Pb incorporation in the undoped AlSb layer, during the growth of which the PbTe source was shuttered, but hot. This background may be due to residual Pb present in the chamber, which evaporates off heated parts of the chamber due to its high vapor pressure and gets incorporated in the sample, or due to Pb in the antimony source. At present, we cannot distinguish between these two possible causes.

CONCLUSIONS

Lead telluride is a controllable source of tellurium for doping GaSb and AlSb. Doping concentrations from 1.2×10^{16} to $1.6 \times 10^{18} \text{ cm}^{-3}$ have been obtained. Tellurium incorporation is a strong function of GaSb growth conditions, so the growth conditions must be carefully controlled. At the flux ratio and temperature required for good-quality GaSb growth, we have obtained good doping efficiencies (about 50% of those in GaAs). Sharp doping profiles can be obtained. Similarly efficient doping of AlSb has also been achieved.

The ability to dope both GaSb and AlSb efficiently does not necessarily carry over to the (Al,Ga)Sb alloys. Recent work by Takeda *et al.*¹⁸ has shown that the DX-center, so prevalent in the (Al,Ga)As system, is also present in the (Al,Ga)Sb alloys. In our own work, presented here, we have investigated only the end-points (GaSb and AlSb) of the (Al,Ga)Sb system, and our results suggest that at the end points the concentration of DX centers is low. We have not yet investigated Te-doping of the (Al,Ga)Sb alloys with PbTe quantitatively, but qualitative observations on $\text{Al}_{0.8}\text{Ga}_{0.2}\text{Sb}$ alloys, by Nakagawa¹⁹ in our laboratory, made in a different context, suggest that already at such a low Al concentration the *n*-type doping of the alloy does indeed become inefficient. However, even if it should turn out that the bulk alloys can not be doped with high efficiency, our results suggest that it should still be possible to obtain a high doping efficiency in superlattice alloys, by replacing the bulk alloy with a selectively Te-doped short-period AlSb/GaSb

superlattice, as demonstrated for the (Al,Ga)As system by Baba *et al.*²⁰

ACKNOWLEDGEMENTS

The authors would like to thank Don Zak and Brian Carralejo for technical assistance, Gayle Lux and Clive Jones for the SIMS measurements, and Ernie Caine for useful discussions. This work was supported by the Office of Naval Research and by the Semiconductor Research Corporation.

REFERENCES

1. C. A. Chang, R. Ludeke, L. L. Chang and L. Esaki, *Appl. Phys. Lett.* **31**, 759, (1977).
2. S. Subbanna and H. Kroemer, unpublished results.
3. M. Yano, Y. Suzuki, T. Ishii, Y. Matsushima and M. Kimata, *Jpn. J. Appl. Phys.* **17**, 2091 (1978).
4. H. Gotoh, K. Sasamoto, S. Kuroda, T. Yamamoto, K. Tamamura, M. Fukushima and M. Kimata, *Jpn. J. Appl. Phys.* **20**, L893 (1981).
5. T. M. Kerr, private communication.
6. D. A. Andrews, M. Y. Kong, R. Heckingbottom and G. J. Davies, *J. Appl. Phys.* **55**, 841 (1984).
7. C. E. C. Wood, *Appl. Phys. Lett.* **33**, 770 (1978).
8. J.-D. Sheng, Y. Makita, K. Ploog and H. J. Queisser, *J. Appl. Phys.* **53**, 999 (1982).
9. T. D. McLean, T. M. Kerr, D. I. Westwood, C. E. C. Wood, D. F. Howell and R. J. Nicholas, paper presented at 6th MBE Workshop, Minneapolis, 1985, unpublished.
10. T. D. McLean, private communication.
11. N. B. Brandt, S. V. Demishev, A. A. Dmitriev, V. V. Moshchalkov, L. N. Parchevskaya and S. M. Chudinov, *Sov. Phys. JETP* **59**, 847 (1984).
12. R. F. Brebrick and A. J. Strauss, *J. Chem. Phys.* **40**, 3230 (1964).
13. A. Y. Cho and J. R. Arthur, *Prog. Solid St. Chem.* **10**, 157 (1975).
14. B. Joyce, *Rep. Prog. Phys.* **48**, 1637 (1985).
15. A. Sagar, *Phys. Rev.* **117**, 93 (1960). See also A. Joulie, A. Zein Eddin and B. Girault, *Phys. Rev. B*, **23**, 928 (1981), and references therein.
16. A. S. Pashinkin and A. V. Novoselova, *Russ. J. Inorg. Chem.* **4**, 1229 (1959).
17. D. A. Andrews, R. Heckingbottom and G. J. Davies, *J. Appl. Phys.* **60**, 1009, (1986).
18. Y. Takeda, Y. Zhu and A. Sasaki, 14th Int'l. Symp. GaAs and Related Compounds, Heraklion, Greece, (1987).
19. A. Nakagawa and H. Kroemer, unpublished results.
20. T. Baba, T. Mizutani and M. Ogawa, *Jpn. J. Appl. Phys.* **22**, 10, L627 (1983).